

## Sandwich Complexes of the Metalloaromatic $\eta^3$ -Al<sub>3</sub>R<sub>3</sub> Ligand

Jose M. Mercero,\* Mario Piris, Jon M. Matxain, Xabier Lopez, and Jesus M. Ugalde

Kimika Fakultatea, Euskal Herriko Unibertsitatea and Donostia International Physics Center (DIPC),  
P.K. 1072, 20080 Donostia, Euskadi, Spain

Received January 19, 2009; E-mail: jm.mercero@ehu.es

The aromaticity of the [Al<sub>3</sub>R<sub>3</sub>]<sup>2-</sup> three-membered dianion ring has recently been put forward by Power and co-workers<sup>1</sup> by means of their remarkable synthesis of the Na<sub>2</sub>[Al<sub>3</sub>R<sub>3</sub>] (R = 2,6-dimesitylphenyl) complex. Examination of the calculated valence molecular orbitals (MOs) revealed an occupied  $\pi$ -type orbital delocalized over the three aluminum atoms, which led them to state that Na<sub>2</sub>[Al<sub>3</sub>R<sub>3</sub>] is aromatic, in accordance with Hückel's  $4n + 2$  rule.

This compound belongs to a family of group IIIB three-membered rings investigated earlier by Robinson and co-workers,<sup>2-5</sup> of which disodium tris((2,6-dimesitylphenyl)cyclogallene), Na<sub>2</sub>[Ga<sub>3</sub>R<sub>3</sub>] (R = Mes<sub>2</sub>C<sub>6</sub>H<sub>3</sub>; Mes = 2,4,6-Me<sub>3</sub>C<sub>6</sub>H<sub>2</sub>), was the first one synthesized.<sup>2</sup> This molecule and its dipotassium congener<sup>3</sup> also possess a stabilizing occupied  $\pi$ -type valence MO that is delocalized over the three gallium atoms. Subsequent analysis of nucleus-independent chemical shift (NICS) values of the model compounds M<sub>2</sub>[Ga<sub>3</sub>H<sub>3</sub>] (M = Li, Na, K)<sup>6</sup> revealed that their [Ga<sub>3</sub>H<sub>3</sub>]<sup>2-</sup> cores are indeed best described as *metalloaromatic*, as this metal ring system exhibits traditional (organic) aromaticity.

The (metallo)aromaticity of the [Al<sub>3</sub>R<sub>3</sub>]<sup>2-</sup> dianions can be explained similarly. In particular, analysis of the canonical molecular orbital NICS (CMO-NICS) values for the optimized structure of the cyclotriallane dianion, [Al<sub>3</sub>H<sub>3</sub>]<sup>2-</sup> (shown in Figure 1), indicates that there are three independent valence MO systems (see the Supporting Information for a detailed account of these calculations). In addition to the already mentioned aromatic  $\pi$ -type system, there are also the aromatic *radial* and the antiaromatic *tangential* systems, which are of the  $\sigma$  type.

It should be noted that the orbitals of the tangential system are arranged in *reverse order*, that is, two degenerate orbitals below one nondegenerate orbital, instead of the *normal order* of one nondegenerate orbital below two degenerate ones. This fact substantially alters the ordinary Hückel-like electron-counting rules and must therefore be treated with care.

Our calculated CMO-NICS values reveal that both the  $\pi$  and radial systems are aromatic while the tangential system is antiaromatic, as in the [Al<sub>4</sub>]<sup>2-</sup> aromatic ring.<sup>7,8</sup> Nevertheless, the [Al<sub>3</sub>H<sub>3</sub>]<sup>2-</sup> dianion is both  $\pi$ - and  $\sigma$ -aromatic, as revealed by the values at 1 Å above and at the ring center, NICS(1) = -11.02 ppm and NICS(0) = -13.04 ppm, respectively (Table 1).

Consequently, the question of whether cyclotriallane rings could be used as ligands for sandwich complexes arises naturally. In this vein, the tendency of small aluminum rings to collapse into clusters with an increased number of Al–Al contacts, as anticipated earlier by Seo and Corbett,<sup>9</sup> constitutes one crucial problem that must be considered before proceeding further.

Voluminous substituents R on the Al<sub>3</sub>R<sub>3</sub> rings can indeed be used to protect aluminum atoms from collapsing. Thus, Schnöckel and co-workers have succeeded in stabilizing the [Al( $\eta^3$ -Al<sub>3</sub>R<sub>3</sub>)<sub>2</sub>]<sup>-</sup> [R = N(SiMe<sub>3</sub>)<sub>2</sub>]<sup>10</sup> and [Al( $\eta^3$ -Al<sub>3</sub>R<sub>3</sub>)<sub>2</sub>]<sup>-</sup> [R = N(SiMe<sub>2</sub>Ph)<sub>2</sub>]<sup>11</sup> sandwich complexes. However, after a careful study of the electronic

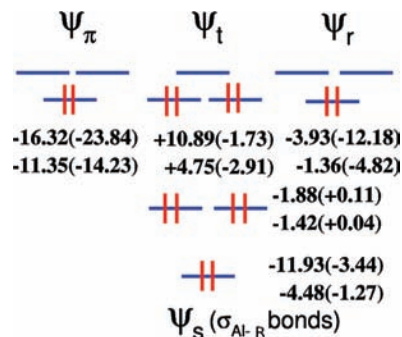


**Figure 1.** CMO-NICS values (ppm) at the ring center (top number in each pair) and 1 Å above the ring center (bottom number in each pair) for [Al<sub>3</sub>H<sub>3</sub>]<sup>2-</sup> and (in parentheses) [Al<sub>3</sub>F<sub>3</sub>]<sup>2-</sup>.

**Table 1.** NICS Values (ppm) at the Ring Center [NICS(0)] and 1 Å above the Ring [NICS(1)] of [Al<sub>3</sub>R<sub>3</sub>]<sup>2-</sup> Along with Al–Al and Al–R Bond Lengths (Å)

R	NICS(0)	NICS(1)	d(Al–Al)	d(Al–R)
F	-45.14	-27.61	2.559	1.708
Cl	-39.50	-29.44	2.531	2.344
Br	-37.30	-23.97	2.527	2.564
CH <sub>3</sub>	-37.25	-21.34	2.528	2.066
NO <sub>2</sub>	-34.06	-22.53	2.519	2.087
CHCH <sub>2</sub>	-22.50	-15.59	2.518	2.040
CF <sub>3</sub>	-26.10	-17.54	2.481	2.136
CN	-21.90	-15.21	2.476	2.049
H	-13.04	-11.02	2.521	1.668

structure of the model compound [Al( $\eta^3$ -Al<sub>3</sub>H<sub>3</sub>)<sub>2</sub>]<sup>-</sup>, they concluded that the [Al<sub>3</sub>R<sub>3</sub>]<sup>2-</sup> fragments should not be described as aromatic systems because of the lack of a ring-current-induced high-field shift for the central Al: the ring-current-induced field shift at the central Al was  $\delta(\text{Al}) = +798$  ppm in [Al( $\eta^3$ -Al<sub>3</sub>H<sub>3</sub>)<sub>2</sub>]<sup>-</sup>, which should be compared with the field induced ( $\delta(\text{Al}) = -114$  ppm) by *real* aromatic rings, as in the aluminumocenium cation, [Al( $\eta^5$ -Cp\*)<sub>2</sub>]<sup>+</sup>.<sup>12</sup> We have estimated the NICS(0), NICS(-1), and NICS(1) values for the [Al<sub>3</sub>R<sub>3</sub>]<sup>2-</sup> rings in [Al( $\eta^3$ -Al<sub>3</sub>H<sub>3</sub>)<sub>2</sub>]<sup>-</sup>; the calculated values (-1.34, -6.47, and -7.68 ppm, respectively) indicate that the aromaticity of the [Al<sub>3</sub>H<sub>3</sub>]<sup>2-</sup> ligands decreases substantially upon complexation, in accordance with the statement of Schnöckel and co-workers.<sup>11</sup>

However, it should be noted that the aromaticity of the cyclotriallane ring should indeed be influenced by the R substituents attached to the aluminum atoms. Consequently, R = H might not be the best substituent if the ring is to retain its aromaticity upon complexation. Even more, it is well-known<sup>13</sup> that the *D*<sub>3h</sub> structure is not the most stable isomer of [Al<sub>3</sub>H<sub>3</sub>]<sup>2-</sup>.

We have indeed found substituents other than hydrogen that render substantially higher aromaticity to the cyclotriallane ring. Thus, inspection of the calculated NICS values shown in Table 1

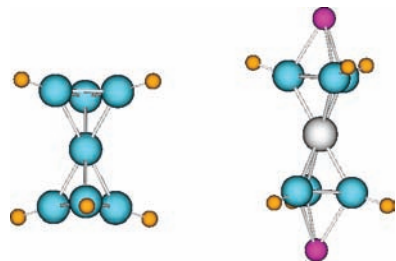


**Figure 2.** Optimized structures of (left)  $[\text{Al}(\eta^3\text{-Al}_3\text{F}_3)_2]^-$  and (right)  $\text{Na}_2[\text{Ti}(\eta^3\text{-Al}_3\text{F}_3)_2]$ . Main geometrical features and NICS values are given in Table 2.

**Table 2.** NICS(0) and NICS(1) Values (ppm) for the  $[\text{Al}_3\text{F}_3]^{2-}$  Rings, Al–Al and Al–R Bond Lengths, and Values of  $d(\text{M}-\text{COR})$ , the Distance (Å) between the Complexed Metal (M) and the Center of the  $\text{Al}_3$  Ring (COR)

complex	NICS(0)	NICS(1)	$d(\text{Al}-\text{Al})$	$d(\text{Al}-\text{R})$	$d(\text{M}-\text{COR})$
$[\text{Al}(\eta^3\text{-Al}_3\text{H}_3)_2]^-$	-1.34	-7.68	2.536	1.612	2.277
$[\text{Al}(\eta^3\text{-Al}_3\text{F}_3)_2]^-$	-24.87	-14.40	2.556	1.690	2.332
$\text{Na}_2[\text{Ti}(\eta^3\text{-Al}_3\text{F}_3)_2]$	-35.51	-22.54	2.604	1.687	2.407
$\text{Na}_2[\text{Mg}_2(\eta^3\text{-Al}_3\text{F}_3)_2]$	-36.84	-18.29	2.603	1.688	2.502
$\text{Na}_2[\text{Zn}_2(\eta^3\text{-Al}_3\text{F}_3)_2]$	-36.49	-21.66	2.606	1.683	2.247

indicates that both  $\pi$  acceptors, such as  $-\text{C}\equiv\text{N}$ , and  $\sigma$  donors, such as  $-\text{CH}_3$ , increase the aromaticity of the cyclotrialane ring relative to that of  $[\text{Al}_3\text{H}_3]^{2-}$ . However, we observe that the largest enhancement of the aromaticity of the ring occurs for halides. In particular, we wish to draw attention to the strong aromatic character of  $[\text{Al}_3\text{F}_3]^{2-}$ , as suggested by its large negative NICS values (also see Figure 1). One can observe that for  $[\text{Al}_3\text{F}_3]^{2-}$ , even the tangential degenerate MOs are slightly aromatic, in contrast to their noticeable antiaromaticity in  $[\text{Al}_3\text{H}_3]^{2-}$ . Additionally, it is worth noticing that in contrast to  $[\text{Al}_3\text{H}_3]^{2-}$ , the  $D_{3h}$  structure is the most stable isomer of  $[\text{Al}_3\text{F}_3]^{2-}$  (see the Supporting Information).

Thus, the structural stability and the large aromatic character, which might be strong enough to prevent aromaticity quenching upon complexation, make the perfluorinated cyclotrialane ring a potentially stable metal-complexing ligand.

We calculated the optimum structure of the  $[\text{Al}(\eta^3\text{-Al}_3\text{F}_3)_2]^-$  sandwich complex, which is shown in Figure 2. The salient geometrical features, along with the NICS values at the center of the cyclotrialane ring and 1 Å above it, are given in Table 2. One can observe that both NICS values are large and negative for  $[\text{Al}(\eta^3\text{-Al}_3\text{F}_3)_2]^-$  in comparison with those of  $[\text{Al}(\eta^3\text{-Al}_3\text{H}_3)_2]^-$ , in spite of the similarity of the Al–Al distances. Therefore, the  $[\text{Al}_3\text{F}_3]^{2-}$  fragments should be seen as aromatic systems even upon complexation.

Complexation of transition metals is illustrated by the charge-compensated  $\text{Na}_2[\text{Ti}(\eta^3\text{-Al}_3\text{F}_3)_2]^{18e^-}$  sandwich complex, for which the optimum structure is shown in Figure 2 and the key magnetic and geometrical properties are collected in Table 2. It should be noted that the aromaticity of the cyclotrialane rings remains when the complex is formed, as revealed by the NICS(0) and NICS(1) values ( $-35.5$  and  $-22.5$  ppm, respectively; see Table 2). The electronic ground state of the complex is the  $^3A_{1g}$  state, which corresponds to a  $D_{3d}$  staggered configuration of the ligands and has the spin density localized on the Ti atom [ $\rho^s(\text{Ti}) = 1.8$ ]. Our calculations therefore predict that the atomic-like magnetism is preserved upon complexation, a fact that could be exploited further in the design of magnetic molecules.

Another likely strategy for preventing the aluminum atoms from aggregation is to use metal dimers as spacers between the two

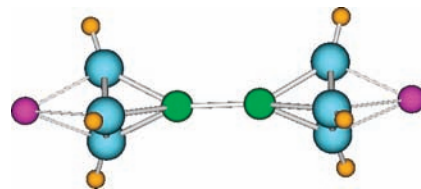


**Figure 3.** Optimized structure of  $\text{Na}_2[\text{Mg}_2(\eta^3\text{-Al}_3\text{F}_3)_2]$ . Color code: cyan, Al; brown, F; green, Mg; magenta, Na.

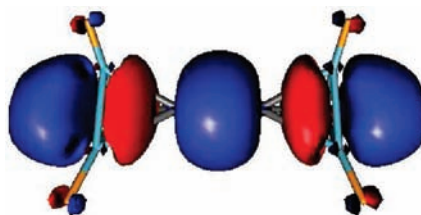


**Figure 4.** Representation of the HOMO of  $\text{Na}_2[\text{Mg}_2(\eta^3\text{-Al}_3\text{F}_3)_2]$ .

cyclotrialane ligand rings in order to place them as far apart from each other as possible. Additionally, as above, one could use electron-withdrawing substituents at the  $\text{Al}_3\text{R}_3$  rings in order to increase the stability of the complexes through inductive and hyperconjugation effects, as shown in Table 1.

Bearing in mind these two facts, we optimized the structure of  $\text{Na}_2[\text{Mg}_2(\eta^3\text{-Al}_3\text{F}_3)_2]$ , shown in Figure 3, and found that the Mg dimer is arranged perpendicular to the two  $\text{Al}_3\text{F}_3$  ring planes, which are parallel and separated by a distance of  $\sim 7.9$  Å. One can observe that the two  $\text{Al}_3\text{F}_3$  rings are eclipsed, while they are staggered in both  $[\text{Al}(\eta^3\text{-Al}_3\text{F}_3)_2]^-$  and  $\text{Na}_2[\text{Ti}(\eta^3\text{-Al}_3\text{F}_3)_2]$ , as shown in Figure 2. Additionally, our calculated NICS values [NICS(0) =  $-36.84$  ppm, NICS(1) =  $-18.29$  ppm] indicate that both  $\text{Al}_3\text{F}_3$  rings remain aromatic upon complexation of the magnesium dimer.

This molecular structure has no negative force constants, and the optimum Mg–Mg bond length is 2.886 Å, which should be compared with the experimental<sup>14</sup> Mg–Mg distance of 2.8508(12) Å for  $\text{Mg}_2[(\text{Ar}'\text{N})_2\text{C}(\text{NMe}_2)_2]$  ( $\text{Ar}' = 2,6\text{-Me}_2\text{C}_6\text{H}_3$ ), the calculated Mg–Mg bond length of 2.763 Å in the recently isolated  $\text{Mg}_2\text{Cl}_2$ ,<sup>15</sup> and the calculated Mg–Mg bond length of 2.809 Å in  $\text{Mg}_2(\eta^5\text{-C}_5\text{H}_5)_2$ ,<sup>16</sup> whose experimental determination constitutes one of the most exciting challenges in main-group organic chemistry.

Figure 4 depicts the highest occupied molecular orbital (HOMO) of  $\text{Na}_2[\text{Mg}_2(\eta^3\text{-Al}_3\text{F}_3)_2]$ , which largely describes a Mg–Mg  $\sigma$ -bonding interaction. Additional hints about the stability of this molecule are found in its large HOMO–LUMO gap of 2.18 eV and the fact that the calculated lowest stretching vibrational frequency has the reasonably large value of  $107\text{ cm}^{-1}$ , in accordance with the criteria given recently by Hoffmann et al.<sup>17</sup>

Likewise, we also optimized the structure of the charge-compensated complex  $\text{Na}_2[\text{Zn}_2(\eta^3\text{-Al}_3\text{F}_3)_2]$ , whose salient geometrical and magnetic properties are summarized in Table 2. The two  $[\text{Al}_3\text{F}_3]$  ligands remain aromatic upon complexation, adopt the eclipsed conformation, and are parallel to each other and separated by 6.96 Å. This can be compared with the distance of 6.4 Å between the  $\text{C}_5(\text{CH}_3)_5$  ligands of the recently synthesized dizincocene  $\text{Zn}_2(\eta^3\text{-C}_5(\text{CH}_3)_5)_2$ .<sup>18</sup> Additionally, the optimized Zn–Zn bond length in  $\text{Na}_2[\text{Zn}_2(\eta^3\text{-Al}_3\text{F}_3)_2]$  is 2.47 Å, which should be compared with the corresponding Zn–Zn bond length in  $\text{Zn}_2(\eta^3\text{-C}_5(\text{CH}_3)_5)_2$ , namely, 2.305 Å (exptl) and 2.34 Å (calcd, B3LYP/6-311+G\*\*).<sup>19</sup>

Finally, in Figure 5 we show the structure of the multiple-decker complex  $\text{Na}_2[(\text{Mg}_2)_2(\eta^3\text{-Al}_3\text{tBu}_3)_3]$ . This molecule illustrates the realization of a number of concepts that could be used in order to

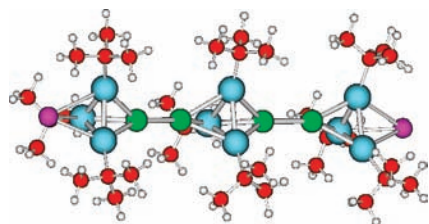


**Figure 5.** Structure of  $\text{Na}_2[(\text{Mg}_2)_2(\eta^3\text{-Al}_3\text{Bu}_3)_3]$ . Color code: cyan, Al; red, C; gray, H; green, Mg; magenta, Na.

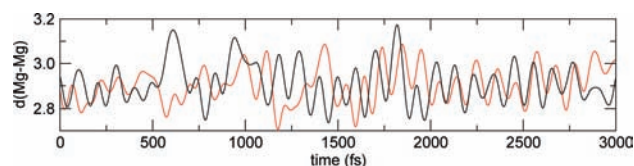


**Figure 6.** Variation of the Mg–Mg bond lengths (Å) in  $\text{Na}_2[(\text{Mg}_2)_2(\eta^3\text{-Al}_3\text{Bu}_3)_3]$  as a function of time.

make sandwich complexes with aromatic  $\text{Al}_3\text{R}_3$  ligands. First, the aluminum atoms have been protected from aggregation by two means: placing longer “spacers” between the  $[\text{Al}_3\text{R}_3]^{2-}$  ligands and using bulky substituents ( $\text{R} = \text{tert-butyl}$  in this case) to impart steric protection. Second, the charge compensation by the terminal alkali cations stabilizes the complex toward electron autodetachment, and the steric hindrance provided by the bulkiness of the R substituents imparts structural stiffness to the complex. Third, the  $[\text{Al}_3\text{Bu}_3]$  ligands possess a large enough aromatic character to remain aromatic upon complexation. Finally, it is worth mentioning that a  $D_{3d}$ -symmetric distorted octahedron  $[\text{Al}_6\text{Bu}_6]^-$  radical anion cluster has been synthesized.<sup>20</sup>

Additionally, it is seen that these complexes can polymerize into longer 1D structures to yield multiple-decker *multimetalocene*-like sandwich complexes, a new class of molecules that on the basis of our calculations seems to be within experimental reach. Our quantum molecular dynamics simulations demonstrate that this 1D structure remains unaltered during the whole simulation time. Concomitantly, Figure 6 shows that the variations of the Mg–Mg distances in each of its two central  $\text{Mg}_2^{2+}$  units remain within the assigned boundaries<sup>14</sup> of the distance in the singly bonded magnesium dimer (i.e., the bond length of diatomic magnesium,  $3.89 \text{ \AA}^{21}$ ) and the sum of two magnesium covalent radii ( $2.72 \text{ \AA}$ ).<sup>22</sup> This is very supportive of the structural stability of the triple-decker  $\text{Na}_2[(\text{Mg}_2)_2(\eta^3\text{-Al}_3\text{Bu}_3)_3]$  sandwich complex.

In summary, we have shown computational evidence of both the structural integrity and the thermal stability of metal coordination complexes containing aromatic  $[\eta^3\text{-Al}_3\text{R}_3]^{2-}$  ligands. Both metal atoms and metal dimers could be sandwiched by conveniently chosen  $[\eta^3\text{-Al}_3\text{R}_3]$  ligands. Starting from this point, chemists could experiment with different R substituents on the  $[\text{Al}_3\text{R}_3]^{2-}$  rings and various ligands that could be attached in the coordination sphere of the sandwiched metal(s). Additionally, voluminous substituents

could be utilized to tune the steric hindrance around the central metal atom(s) and hence to increase the stability of the complex. Finally, it is recognized that both ligand attachment mechanisms and reactivity patterns in the coordination sphere of the central atoms(s) represent unexplored exciting corners of the chemistry of these novel sandwich complexes, which have not yet been prepared. However, it is anticipated that the first experimental hint of such species may come from gas-phase investigations (e.g., using FT-ICR mass spectrometry).<sup>23</sup>

**Acknowledgment.** This research was funded by Eusko Jauriaritza (the Basque Government) and the Spanish MCyT. The SGI/IZO-SGIker UPV/EHU is acknowledged for computational resources.

**Note Added after ASAP Publication.** In the first paragraph there was an error in the version published ASAP May 4, 2009; 2,6-diphenylphenyl was corrected to 2,6-dimesitylphenyl in the version published on the web May 20, 2009.

**Supporting Information Available:** Coordinates and simulated IR spectra for all of the structures described in the text. This material is available free of charge via the Internet at <http://pubs.acs.org>.

## References

- (1) Wright, R. J.; Brynda, M.; Power, P. P. *Angew. Chem., Int. Ed.* **2006**, *45*, 5953.
- (2) Li, X. W.; Pennington, W. T.; Robinson, G. H. *J. Am. Chem. Soc.* **1995**, *117*, 7578.
- (3) Li, X. W.; Xie, Y.; Schreiner, P. R.; Gripper, K. D.; Crittendon, R. C.; Campana, C. F.; Schaefer, H. F., III; Robinson, G. H. *Organometallics* **1996**, *15*, 3798.
- (4) Robinson, G. H. *Acc. Chem. Res.* **1999**, *32*, 773.
- (5) Wang, Y.; Robinson, G. H. *Organometallics* **2007**, *26*, 2.
- (6) Xie, Y.; Schreiner, P. R.; Schaefer, H. F., III; Li, X. W.; Robinson, G. H. *J. Am. Chem. Soc.* **1996**, *118*, 10635.
- (7) Chen, Z.; Corminboeuf, C.; Heine, T.; Bohmann, J.; Schleyer, P. v. R. *J. Am. Chem. Soc.* **2003**, *125*, 13930.
- (8) Islas, R.; Heine, T.; Merino, G. *J. Chem. Theory Comput.* **2007**, *3*, 775, and references therein.
- (9) Seo, D.-K.; Corbett, J. D. *Science* **2001**, *291*, 841.
- (10) Purath, R.; Köppe, R.; Schnöckel, H. *Angew. Chem., Int. Ed.* **1999**, *38*, 2926.
- (11) Yang, P.; Köppe, R.; Duan, T.; Hartig, J.; Hadiprono, G.; Pilawa, B.; Keilhauer, I.; Schnöckel, H. *Angew. Chem., Int. Ed.* **2007**, *46*, 3579.
- (12) Dohmeier, C.; Schnöckel, H.; Schneider, U.; Ahlrichs, R.; Robl, C. *Angew. Chem., Int. Ed.* **1993**, *32*, 1655.
- (13) Srinivas, G. N.; Anoop, A.; Jemmis, E. D.; Hamilton, T. P.; Lammertsma, K.; Leszczynski, J.; Schaefer, H. F., III. *J. Am. Chem. Soc.* **2003**, *125*, 16397.
- (14) Green, S. P.; Jones, C.; Stasch, A. *Science* **2007**, *318*, 1754.
- (15) Köppe, R.; Henke, P.; Schnöckel, H. *Angew. Chem., Int. Ed.* **2008**, *47*, 8740.
- (16) Velázquez, A.; Fernández, I.; Frenking, G.; Merino, G. *Organometallics* **2007**, *26*, 4761.
- (17) Hoffmann, R.; Schleyer, P. v. R.; Schaefer, H. F., III. *Angew. Chem., Int. Ed.* **2008**, *47*, 7164. See, however, the response of Prof. Frenking: Frenking, G. *Angew. Chem., Int. Ed.* **2008**, *47*, 7168.
- (18) Resa, I.; Carmona, E.; Gutierrez-Puebla, E.; Monge, A. *Science* **2004**, *305*, 1136.
- (19) Carmona, E.; Galindo, A. *Angew. Chem., Int. Ed.* **2008**, *47*, 6526–6536.
- (20) Dohmeier, C.; Mocker, M.; Schnöckel, H.; Löt, A.; Schneider, U.; Ahlrichs, A. *Angew. Chem., Int. Ed.* **1993**, *32*, 1428.
- (21) Huber, K. P.; Herzberg, G. *Constants of Diatomic Molecules*; Van Nostrand: New York, 1979; pp 116, 394.
- (22) Emsley, J. *The Elements*, 2nd ed.; Clarendon: Oxford, U.K., 1995.
- (23) Koch, K.; Burger, R.; Stösser, G.; Schnöckel, H. *Eur. J. Mass Spectrom.* **2005**, *11*, 469.

JA8095043